Spaceflight altered the gene and protein expression of the membrane transporter proteins in Jurkat cells

[1]Sue-Mian Then†, [1]Fazlina Nordin‡, [1]Khairul-Bariah Ahmad Amin Noordin*, [1]Hafidzah Munajat, [2]Noor-Hamidah Hussin, [3]Maha Abdullah, [4]David Klaus, [5]Louis Stodieck, [1]Rahman Jamal

[1]1UKM Medical Molecular Biology Institute (UMBI), UKM Medical Centre, 56000 Cheras, Kuala Lumpur, Malaysia; [2]Dept of Pathology, Faculty of Medicine, Universiti Kebangsaan Malaysia (UKM), UKM Medical Centre, 56000 Cheras, Kuala Lumpur, Malaysia; [3]Dept of Pathology, Faculty of Medicine, Universiti Putra Malaysia (UPM), 43400 UPM Serdang, Selangor, Malaysia; [4]Aerospace Engineering Science, University of Colorado, USA; [5]BioServe Space Technology, University of Colorado, USA
*†Current Address: School of Pharmacy, Faculty of Science and Engineering, University of Nottingham Malaysia Campus, 43500 Semenyih, Selangor, Malaysia; ‡Current Address: Cell Therapy Centre (CTC), Faculty of Medicine, Universiti Kebangsaan Malaysia (UKM), UKM Medical Centre, 56000 Cheras, Kuala Lumpur, Malaysia; *Current Address: School of Dental Sciences, Universiti Sains Malaysia (USM), 16150 Kubang Kerian, Kelantan, Malaysia*

Received on 18/06/2019 / Accepted on 4/11/2020

ABSTRACT

We postulated that spaceflight and microgravity may cause changes to cell membrane structure, therefore affecting the expression of drug transporter proteins. We investigated the global gene expression changes and the expression of multidrug resistance proteins in space-flown Jurkat cells. Fluid Processing Apparatus (FPAs) were used in this study. A set of FPAs was prepared as ground controls (F_Ground) and fixated shortly after launching. The flight samples were flown on the Soyuz TMA-11 and fresh medium were added shortly after docking in the ISS. After 30 minutes, another set of FPAs was added fixative (F_T_0) meanwhile another set were fixed after 72 hours incubation at 37°C (F_T_{72}). The number of cells increased from F_Ground to F_T_0 and to F_T_{72}. Post-flight analysis found that only expression of CD3, MRP1(ABCC1) and BCRP(ABCG2) showed significant changes. The flight samples showed a decrease in MRP1(ABCC1) expression at F_T_{72} compared to F_T_0. Expression of BCRP was also significantly decreased in flight samples compared to F_Ground. qRT-PCR results showed that MRP1(ABCC1) mRNA expression complement with the protein expression but mRNA of BCRP(ABCG2) showed different expression from the protein expression. Microarray analysis showed that the voltage-gated K^+ channel gene, Kv.1 was differentially expressed at different time points. We suggest that cellular membrane adapted to spaceflight by modulating the expression of membrane transporter proteins. These findings shed light to the important role of multidrug resistance proteins for drug efflux, biomolecule transport and pharmacokinetics as there is an increasing need to understand how medicine reacts in the human body under microgravity.

Introduction

Critical medical situation requiring drug treatment may occur during space mission, however microgravity condition during spaceflight may alter the pharmacokinetics and pharmacodynamics of the drugs (1). A recent review showed that medications that was brought to space increased from 10 in 1965 to 107 in 2017 (2). With the current trend of long-term space mission to Mars and the availability of commercial spaceflight in the near future means that there is a need to better understand the cellular and structural changes of the cell and how medicines are metabolized and transported under microgravity conditions are instrumental as there will be increasing demand to bring more medications to space (2). Multidrug resistance (MDR) transporters are transmembrane proteins that utilize adenosine triphosphate (ATP) to translocate various substrates across membranes, plays important roles in physiology process and in drug pharmacokinetics, pharmacodynamics and drug-to-drug interactions (3). The MDR proteins including P-glycoprotein, P-gp (ABCB1), Multi-drug Resistance related Proteins 1,MRP1 (ABCC1), MRP 3 (ABCC3), MRP 4 (ABCC4), Lung Resistance Protein,LRP and Breast Cancer Resistance Protein, BCRP (ABCG2) are involved in multidrug resistance of cancers and bacteria, plus a range of other inherited human diseases (4-6). Membrane transporters such as ATP-

Correspondence to: rahmanj@ppukm.ukm.edu.my; Sue-Mian Then and Fazlina Nordin contributed equally to the work of this paper.

binding-cassette (ABC) transporters and voltage-gated ion channels which are located at the cellular membrane are postulated to undergo remodeling under microgravity. A recent study on global gene and miRNA expression of proliferating human fibroblast cells after 3 days incubation revealed the upregulation of 2.3-fold of the P-gp gene expression between space flown cells and ground control cells. However, there were no significant difference when the same comparison were made between cells that have been in space for 14 days. The study concluded that spaceflight affect the cells at proliferating stage, however more studies are needed to validate the observation.(7) Another study has shed some clue to this, demonstrating reduced MRP2 (ABCC2) transport activity of estradiol 17-β-glucuronide (E17βG) in microgravity during parabolic flights (8). Studies have shown that microgravity altered the ion channels, such as porin in E. coli, which are located at the membrane layer of the cells (9). P-gp (ABCB1) and cytochrome P450 levels were altered in the kidney of murine model under simulated microgravity studies (10) while gene expression studies in microorganisms (Salmonella sp. and Candida sp.) found upregulation of certain ABC transporter genes during short term spaceflight mission (11, 12). Simulated microgravity has also been shown to cause differential activation of K+ channels in vascular smooth muscle cells (9, 13). However, how microgravity affects these MDR proteins and ion channels in human T-cell acute lymphoblastic leukemia (T-ALL) cell line, i. e. Jurkat cells have yet to be investigated.

The Jurkat cells have been used extensively in many microgravity investigations including real space flight and simulated microgravity conditions (14-17). Previous studies have shown that the microtubules of Jurkat cells were altered in microgravity with increased condensation of nuclear DNA, which is one of the characteristics of apoptosis (14). Previous reports also showed that most of the cytoskeletal genes identified such as myosin light polypeptide (MYL5), plectin (PLEC), ankyrin, calponin, tropomodulin and dyactin were up-regulated in space-flown Jurkat (15). Spaceflight has also been shown to alter the human immune system with decreased numbers of T-lymphocytes and natural killer cells in post-flight conditions while there is reduced growth activation and decline in growth rate of the cells total population (16). The activity of natural killer cells were also shown to be reduced at post-flight (18). The intracellular distribution of protein kinase C (PKC) in human leukocytes varied in proportion to the applied g level which showed the cells' ability for gravisensing (19) and cytoskeleton is sensitive to gravity by responding to the altered gravity conditions (20).

Given that the location of the drug transporter proteins and ion channels are at the cell membrane, as well as reported reduction of intracellular ATP in simulated microgravity (21), we postulated that microgravity and any perturbation to the membrane structure during launching might result in changes to the expression of these drug transporter proteins and ion channels. The main objective of this study was to investigate the effects of spaceflight and microgravity on the gene expression, particularly the changes on the plasma membrane such as the MDR proteins and ion channels. The understanding of how spaceflight affects these transmembrane proteins, especially graviperception on the molecular level are crucial as we have yet to understand how cells perceive and adapt to spaceflight and microgravity. We determined the expression of the MDR proteins and their corresponding mRNA expression level as well as gene expression changes of ion channels when the Jurkat cells were exposed to the microgravity condition in the International Space Station (ISS) between different time points compared to the ground controls, namely pre-flight which is 56 hours prior to launching (F_Ground), during docking at ISS which was designated as 0 hour of spaceflight (F_T0) and 72 hours of spaceflight (F_T72).

Materials and methods

Hardware

The Fluid Processing Apparatus (BioServe, USA), which has three levels of biosafety containment, was the hardware used in this experiment. The Fluid Processing Apparatus (FPA) is a syringe-like equipment with a cylindrical glass container within. The glass cylinder has three compartments (denoted as C, M and F compartments as shown in Figure 1) separated by 2 rubber septa and a bypass at the M compartment. The C, M and F compartments were loaded with cells suspended in media, fresh media and fixative respectively which has been previously described [22].

Cell culture

The human lymphoblastic cell line Jurkat clone E6-1, was obtained from the American Type Culture Collection (Rockville, MD, USA) and certified free of mycoplasma contamination by ATCC. Jurkat cells were grown in culture medium consisted of RPMI 1640 (PAA Laboratories GmbH, Austria) supplemented with 10% heat inactivated FCS (PAA Laboratories GmbH, Austria), 2mM glutamine, and

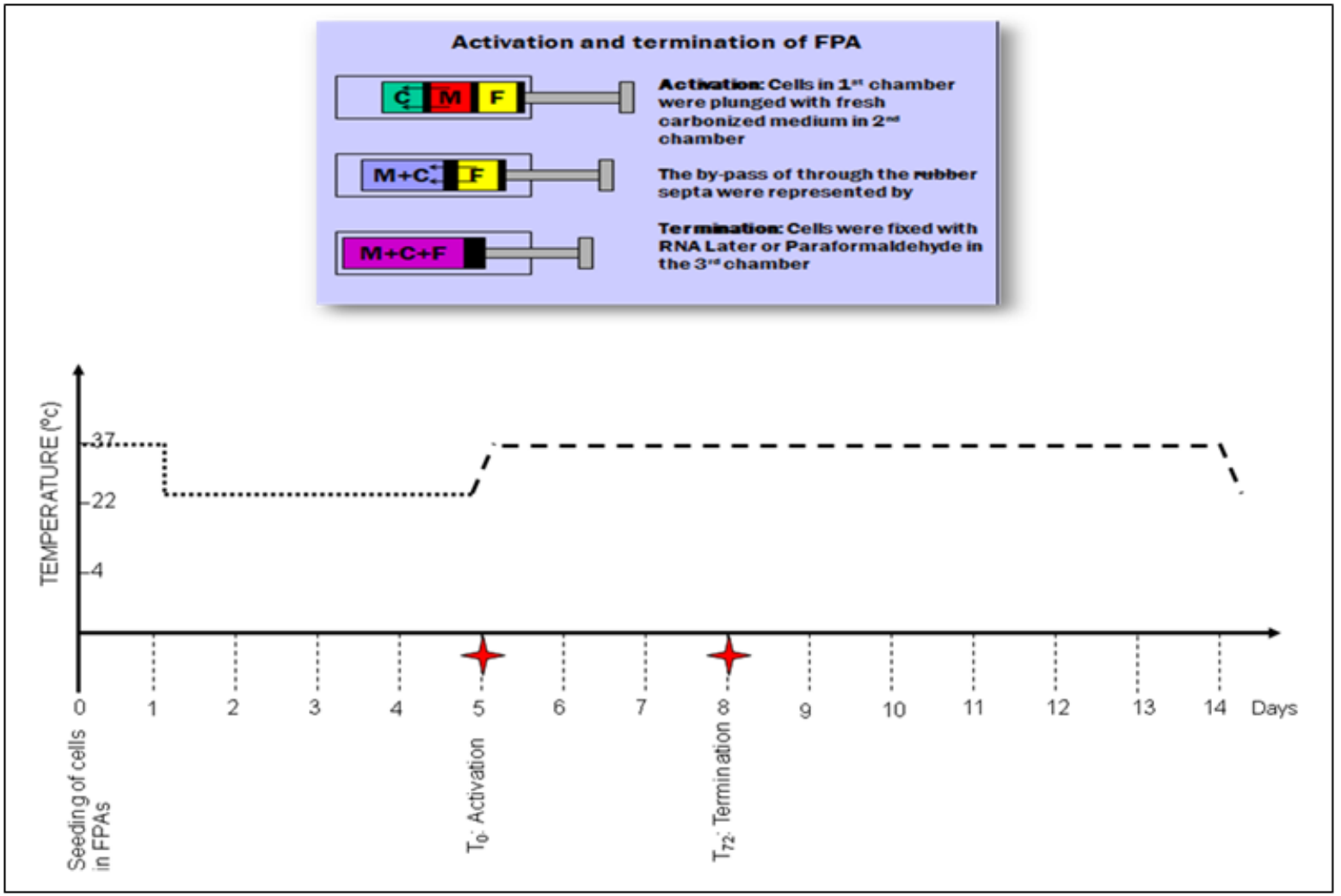

Figure 1
Schematic drawing of the experimental design for the preliminary study to simulate the actual spaceflight conditions that the cells were subjected. Jurkat cells were cultured in either carbonized RPMI 1604 supplemented medium or serum free medium in the FPAs and were subjected to conditions similar to the actual pre-launching and spaceflight conditions as shown in the drawing to study the growth path and viability of the cells.

Correspondence to: rahmanj@ppukm.ukm.edu.my; Sue-Mian Then and Fazlina Nordin contributed equally to the work of this paper.

penicillin and streptomycin, 100 units and 100µg/ml respectively PAA Laboratories GmbH, Austria). Cells were transported using the Opticell™ (Becton Dickinson, USA) to the Institute for Biomedical Problems (Moscow, Russia) and subsequently flown to the laboratory facilities in Baikonur (Kazakhstan) and maintained under optimal growth conditions prior to loading into the FPA. The same passages of cells were used in all test ground and flight experiments.

Optimization of cell culture conditions and simulation ground experiments

The usage of the FPAs for the microgravity experiments provided us with a unique challenge to maintain optimum culture conditions for the Jurkat cells which deviates from the usual cell culture protocol. To counter the lack of CO2 exchange in the FPA, we utilized 4-(2-hydroxyethyl)-1-piperazineethanesulfonic acid (HEPES) and carbonized the medium to provide adequate CO32+ buffering for the cells. We also wanted to study the growth curve of the cells as we anticipated that the cells will be subjected to sub-optimal conditions (during launch and orbiting prior to docking) such as temperatures below 37□C before the transfer after docking to the Kryogem incubator in the ISS as shown in Figure 1. Repeated simulation and optimization of the cell culture conditions were conducted. Jurkat cell suspension (1.5x106 cells/ml) were cultured in 3ml of either carbonized RPMI 1640 (supplemented with L-Glutamine, Pen/Strep and 10% inactivated FCS) or serum free medium (previously described in (5)) in compartment C. Meanwhile, compartment M was filled with 1.5mL of carbonized RPMI 1640 complete growth medium or serum free medium and compartment F was filled with 1.5mL of either 2% paraformaldehyde or RNALater as fixative. After the preparation of cells in the FPAs, the FPAs were kept overnight at 37□C and subsequently subjected to these conditions: 4□C, 37□C and control (which were kept at constant 37□C in non-carbonized medium with CO2 exchange) for 5 days prior to addition of fresh medium and subject the FPAs to 37□C. Cell growth and survival in the different medium and different initial temperature conditions were stained with calcein-AM for detection of live cells while 7-amino Aatinomycin D dye (7-AAD) was used for detection of dead cells and were analyzed using FACS Calibur flowcytometer (BD Bioscience, USA).

Spaceflight experimental details

The preparation of the samples for the spaceflight was performed at the cell culture laboratory in Baikonur, Kazakhstan. The experiments were prepared in triplicates and each FPA was loaded with Jurkat cell suspension (1.5x106 cells/ml) in 3ml of carbonized RPMI 1604 (supplemented with L-Glutamine, Pen/Strep and 10% inactivated FCS) in compartment C, 1.5ml of carbonized RPMI 1604 in compartment M and 1.5ml of either 2% paraformaldehyde (for flowcytometry) or RNALater (for microarray and RT-PCR) in compartment F. The FPAs were tested for leaks prior to being packed into a Nomax bag and handed over to the flight authorities 12 hours before launching on the 10th October 2007. The space vehicle docked on the ISS on the 12th October, 56 hours after the launching and the FPAs were transferred to the Kryogem incubator (set at 37□C) shortly after docking. The cells were then activated by the Malaysian astronaut by pushing the plunger (using a plastic glove box) hence mixing the fresh media from compartment M into compartment C which contained the cells. Once activated the FPAs were returned to the Kryogem and incubated for 72 hours. The experiment was terminated by adding the fixative (either 2% paraformaldehyde or RNALater) from compartment F into compartment C through the bypass. The process of activation and termination of the each FPA were carried out at the following timepoints: F_Ground is when FPAs were activated and fixed consequentially right after launching of the flight mission as baseline controls; F_T0 is when the FPAs were activated in the ISS and fixed consequentially one day after docking at ISS while F_T72 is where FPAs were activated one day after docking but were fixed 72 hours later. All experiments are prepared in triplicates. The detailed time and temperature log of the spaceflight samples were shown in Figure 2.

Flowcytometry analysis of MDR proteins

Detection of P-gp (ABCB1), MRP1 (ABCC1), MRP3 (ABCC3), MRP4 (ABCC4), BCRP (ABCG2) and LRP expressions

To detect the expression of MDR and LRP proteins in the spaceflight samples, the cells were washed with phosphate- buffered saline (PBS, pH 7.4) to wash away the paraformaldehyde. For analysis of each protein, different tubes with 100µL of cells suspension in PBS (1 x 106 cells/mL) were prepared and incubated in permeabilization buffer (eBioscience, USA) for 5 minutes at room temperature. This was followed by the addition of 8µL of monoclonal antibodies which were purified mouse anti-human monoclonal antibody anti-MRP1 (ABCC1) (Clone QCRL1 -from MerckMillipore, USA), purified rabbit anti-human antibody anti-MRP4 (ABCC4) (Clone H-280 from Santa Cruz Biotechnology, USA), purified mouse anti-human antibody anti-MRP3 (ABCC3)

Correspondence to: rahmanj@ppukm.ukm.edu.my; Sue-Mian Then and Fazlina Nordin contributed equally to the work of this paper.

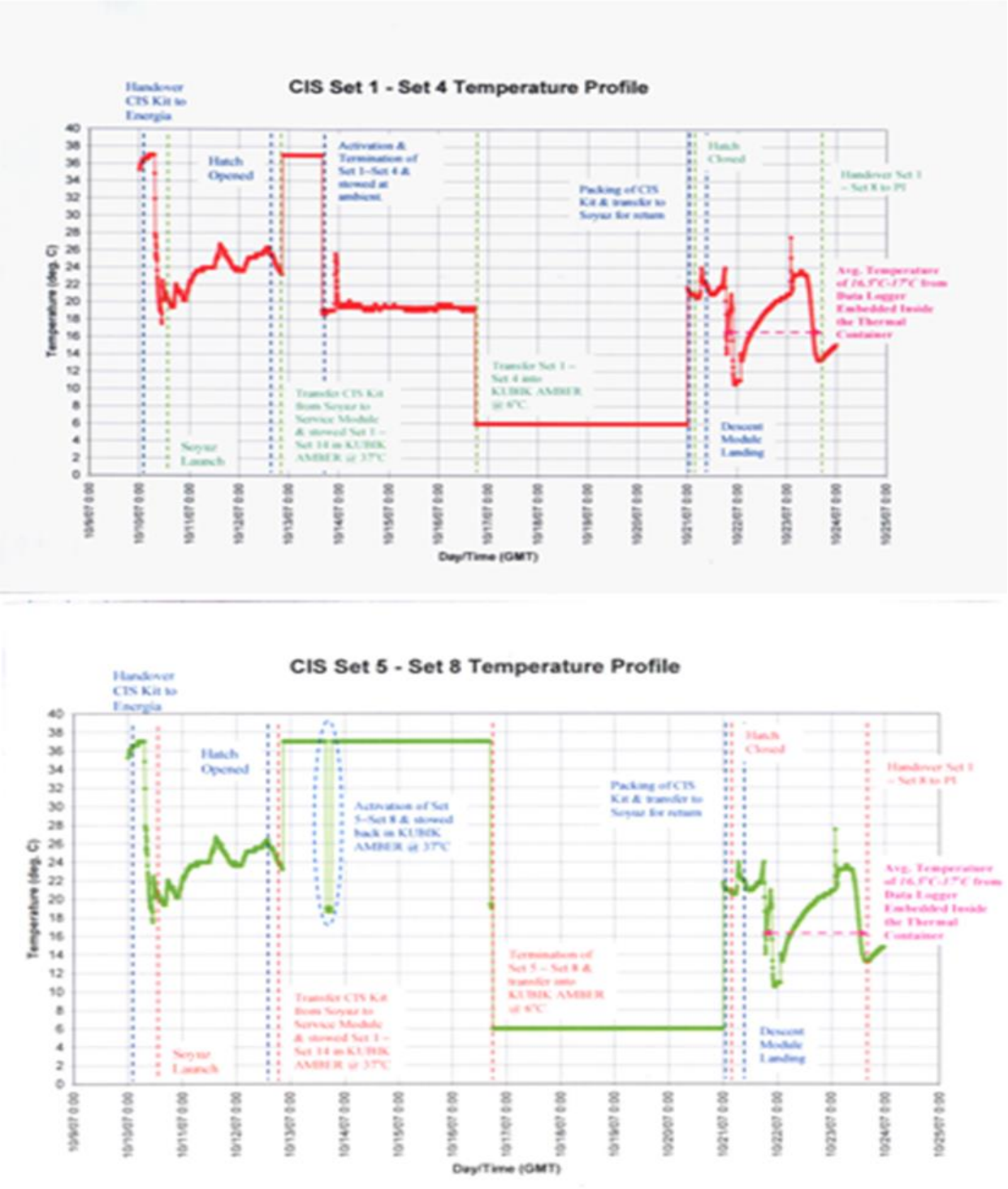

Figure 2. Time and temperature log of the spaceflight samples in the ISS provided National Space Agency (NASA).

Correspondence to: rahmanj@ppukm.ukm.edu.my; Sue-Mian Then and Fazlina Nordin contributed equally to the work of this paper.

(Clone M3II-21 from Abcam, UK) and purified mouse anti-human monoclonal antibody anti-LRP (Clone 42 from BD Bioscience, USA) in each appropriate tube and incubated for 20 minutes in dark at room temperature. After washing with permeabilization buffer, the secondary antibodies were added respectively for each samples which were 1µL (0.2 µg/ µL) of Goat anti-mouse (PE), 1µL (0.2 µg/ µL) of Goat anti-rat (FITC) and 2µL (0.1 µg/ µL) of Goat anti-mouse (FITC) and incubated for 20 min in dark at room temperature. Then the samples were washed with staining buffer (eBioscience, USA) and 10 µL of PE-conjugated anti-CD3 (Clone SP34-2 from BD Bioscience, USA) were added and incubated for another 20 minutes in the dark at room temperature. For the other two monoclonal antibodies, the same amount of cells were stained by using double immunostaining procedure combining surface staining with PE-conjugated anti-CD3 (Clone SP34-2 from BD Bioscience, USA), with FITC-conjugated purified mouse anti-human monoclonal antibody anti-P-gp (Clone 17F9 from BD Bioscience, USA) and FITC-conjugated mouse anti-human monoclonal antibody anti-BCRP (Clone 5D3 from MerckMillipore, USA) which was done separately for each MDR protein. The cells were incubated for 20 minutes in the dark at room temperature. Finally the cells were washed with staining buffer and then kept in 500 µL staining buffer before being analyzed by flowcytometer (FACScan, BD, USA) using CellQuest Pro™ software (FACScan, BD, USA). At least 10,000 events were analyzed for each sample. Unstained samples from each condition were used as controls in all assays.

Total RNA isolation/extraction

Total RNA was extracted and purified using the PARIS kit (Ambion, Japan) according to the manufacturer's protocol and quantified by NanoDrop ND-1000 (Thermo Fisher Scientific, USA). RNA integrity was assessed by micro capillary electrophoresis 2100 Bioanalyzer (Agilent, USA). Samples were then subjected to microarray analysis and RT-PCR.

RNA processing and Hybridization

The RNA samples were converted to double stranded cDNA using the WT-Ovation™ Pico RNA Amplification System (NuGEN Technologies, Inc., USA and subsequently to ST-cDNA using WT-Ovation™ Exon Module (NuGEN Technologies, Inc., USA) before being labeled with FL-Ovation™ cDNA Biotin Module V2 (NuGEN Technologies, USA) according to the manufacturer's protocol. The cDNA were then hybridized on the WT HuGene 1.0 ST Array (Affymetrix, USA). Hybridization results were scanned using the GeneChip Scanner and stored in the GeneChip Operating Software (GCOS).

Microarray data analysis

The Partek Genomics Suite Software 6.4 (Partek Inc, USA) was used for unsupervised analyses as well as gene set enrichment analysis (GSEA) to elucidate the biological pathways or cellular components affected by the two parameters set in this analysis, namely the conditions and the time points. The data which was in the CEL format was normalized by quantile normalization and exploratory analysis was performed using principal component analysis (PCA) scatter plot. Then inferential statistics was performed using ANOVA by setting the p-value less than 0.05 and fold change more than 1.1.

Quantitative real-time PCR (qRT-PCR)

50ng of RNA were converted to cDNA using WT-Ovation™ Pico RNA Amplification System (NuGEN Technologies, USA) according to the manufacturer's protocol. Quantitative real time PCR was performed using the Rotor-Gene™ 6000 (Qiagen, USA). PCR amplifications were performed using QuantiTect® SYBR® Green PCR kit (Qiagen, USA) PCR reactions were performed using 1µl of cDNA in a 25µl total volume reaction containing 12.5µl of 2x QuantiTect® SYBR® Green Master Mix (Qiagen, USA) and 0.3µM final concentration of each primer. PCR reactions were carried out in 0.2µl tubes in Rotor-Gene™ 6000 with 15min PCR initial activation step followed by 40 cycles of 15s at 94°C, 30s annealing and amplification at 72°C. Analysis was performed using the Rotor-Gene™ 6000 software program (Qiagen, USA). A ten-fold dilution series of ground control (F_Ground) cDNA was generated to determine the amplification efficiency of each primer pair. The threshold crossing (Ct) value for each reaction was determined and the fold-change (ΔΔCt value) was calculated with the following formulas using GAPDH as a reference control (23). Primers for quantitative PCR were designed using Primer3 software (24). All primer pairs produced single amplification products as determined by gel electrophoresis as well as melt-curve analysis using the Rotor-Gene™ 6000 software program. Primers used were: GAPDH (forward) 5'-AGGCTGTGGGCAAGGTCATC-3', GAPDH (reverse) 5'-CGCCTGCTTCACCACCTTCT-3', MRP1 (forward) 5'-AAGCAGCCGGTGAAGGTTGTGT-3', MRP1

Correspondence to: rahmanj@ppukm.ukm.edu.my; Sue-Mian Then and Fazlina Nordin contributed equally to the work of this paper.

(reverse) 5'-GCGGCCCGGAAAACATCATCA-3', BCRP (forward) 5'-AACCTGGTCTCAACGCCATC-3', and BCRP (reverse) 5'GTCGCGGTGCTCCATTTATC-3', KCNA1 (forward) 5'-TTTGCCGAGGCGGAAGAAGC-3', KCNA1 (reverse) 5'-AGCCCACGATCTTGCCTCCAC-3'.

Statistical analysis

Statistical analysis of the flowcytometry results was performed using the GraphPad Prism 5 software. The correlations between variables and the significance evaluation were analyzed using two-way ANOVA and the Bonferroni post-test method. A p value of less than 0.05 was considered to be statistically significant.

Results and Discussion

Ground simulation and optimization showed re-growth of cells after activation by addition of fresh medium

The ground simulation experiments showed that although the number of viable cells maintained in 10% FCS dropped after five days in the FPA (this simulated the time period after loading, launching and then in orbit before docking as shown in Figure 1), the cells were able to re-proliferate after the addition of fresh medium and incubation at 37ºC (this simulated the activation at F_T0) after which the cell population peaked at 72 hrs after the addition of medium at 37ºC [Fig. 3 A]. The optimum rate of re-growth were for cells kept initially at 4ºC and this served as the basis for our decision to fix the cells at T72 to capture events at the peak of cell proliferation. This concurred with a previous study that reported low temperature was able to maintain cell viability; this is known as "pausing" cultivated cells, and cells could be maintained for days or weeks at temperature below 37ºC. The study showed that cultured adherent cell line-Chinese Hamster ovary cells (CHO-DG44) and suspension cell line human embryonic kidney cells (HEK293 EBNA) paused at 4ºC for up to 9 days were able to resumed exponential growth at 37ºC (25). In serum free medium, the cells proliferated after three days of seeding in FPA but the viable cells were not able to re-proliferate after addition of fresh medium at 37ºC [Fig. 3 B]. This suggested that usage of FCS that contains growth factors and nutrients was needed for the cells' re-proliferation. Previous study has demonstrated that serum deprivation will cause decreased in cell proliferation and FCS has been shown to enhance proliferation rate (26). These ground simulation experiments established the suitable culture conditions for optimal cell survival and re-growth for the actual spaceflight experiments.

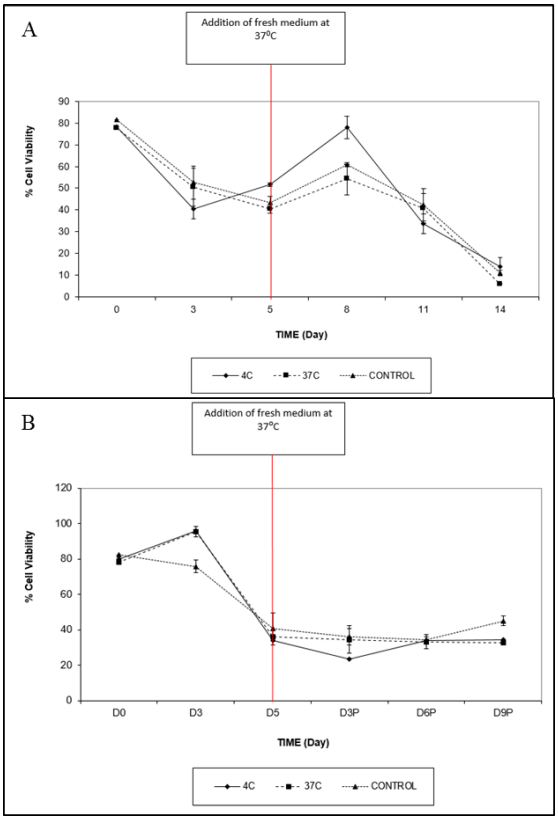

Figure 3: Comparison of Jurkat cells' viability and cell re-growth as assessed by flowcytometry, in which cells were cultured in either (A) carbonized RPMI 1604 supplemented medium or (B) serum free medium, loaded into FPAs and subjected to conditions as described in Materials and Methods. From the result shown, cells that were kept at the initial 4ºC in carbonized RPMI 1604 supplemented medium had the best cell viability and re-growth pattern compared to the rest. Although the viability of cells were the lowest at day 3, but after subsequent addition of fresh medium at 37ºC at day 5, the cell viability improved and peaked after 72 hours at day 8. Therefore, from this result, we are able to simulate the optimal conditions for cell survival during pre-launching and spaceflight condition.

The number of cells increased in flight samples compared to ground controls

Figure 4 showed that there was exponential growth of cells during the spaceflight experiment. The cells were counted (without taking into account whether the cells were viable or not) by using a hemacytometer. The increased numbers of cells from F_Ground to F_T0 and to F_T72 indicated that the cells proliferated even under the stressful conditions of launching (F_T0) as

well as in microgravity condition (F_T72). This data concurred with previous study (14) which showed that Jurkat cells were able to overcome the initial lag in growth in the first few days in microgravity, and some of the cells populations resumed their growth after resupply of nutrients. The cells showed the ability to recover and survive in the harsh conditions (e.g: gravitational changes, suboptimal temperature and etc) of launching and the orbiting without additional medium prior to docking. Another study reported that the Jurkat cell growth curve were not significant affected by simulated launch centrifugal acceleration (3g for 8 minutes) after 24hr and 48 hr, incubation suggested that the hypergravity did not affect growth of Jurkat cells (27). We have also established an optimal protocol to study cell lines in microgravity taking into account the proliferation of the cells and fixating the cells at the time point which will have the highest cell number.

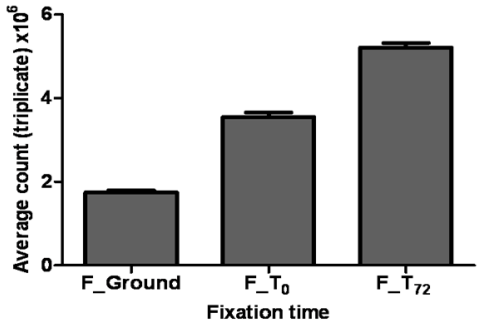

Figure 4. Comparison number of cells of ground (F_Ground) and flight (F_T0 & F_T72) after 4 days and 7 days in microgravity. Cells were maintained at ambient temperature 4°C on carbonized medium containing 10% fetal bovine serum during launch and pre-docking. Flight_Ground indicates that the cells were activated with fresh media at ground level during the launching and immediately after activated the cells was terminated by fixing with formaldehyde. After docking at ISS, FPAs labeled as Flight_T0 were activated with fresh media and a few minutes later, the cells were terminated and as for Flight_T72 the cells were activated and terminated after 72 hours of incubation at 37°C. The data represent the average of triplicates samples from each condition and time.

Altered CD3 marker expression

The CD3-antigen receptor complex has a key role in T-cell recognition and in transmembrane signaling (28). Previous studies have reported that the signal transduction processes were sensitive to microgravity, especially those mediated through protein kinase C (PKC) isoforms (19, 29, 30). From our flowcytometry results [Fig. 5 A], the percentage of cells that expressed the CD3 marker differed at every condition and time point. At F_Ground, the CD3 marker showed 75.8% expression and the percentage increased to 97.2% at F_T0 followed by a decrease to 71.5% at F_T72. The increase in the expression of CD3 at F_T0 (this is after docking) could be related to the stress responses after launching (possibly due to hypergravitation during and after launching) as well as the non-ideal conditions (suboptimal temperature, lack of fresh medium replacement) during orbiting prior to docking. We postulate that this trend in the expression of CD3 may be due to involvement of PKC. This is based on previous study by Matsuda (1994) (31), who reported that activation of PKC will down-regulate the CD3 expression. Others have reported that PKC varies in its intracellular distribution and quantity according to the g level where PKC was increased in spaceflight compared to 1g on the ground and even more increased at hypergravity (1.4g) (32).

Decreased expression of MRP1 and BCRP in microgravity condition

For the MDR proteins analyzed, only MRP1 (ABCC1) and BCRP (ABCG2) showed significant differential expression [Fig. 5 A and Fig. 5 B]. The percentage of cells that expressed MRP1 (ABCC1) decreased significantly from 94.1% at F_T0 to 75% at F_T72. Meanwhile, the expression of BCRP (ABCG2) for flight samples also decreased at both F_T0 (13.4%) and F_T72 (4.8%) compared to the expression at F_Ground (49.0%). Both MRP1 (ABCC1) and BCRP (ABCG2) showed the same trend of decreased expression at microgravity condition especially at F_T72 suggesting that the gravitational changes during spaceflight, including hypergravitation during launching and docking, as well as exposure to microgravity and space radiation may have some effects towards the MDR proteins expression. This result concurred with a recent study which showed significantly reduced MRP2 (ABCC2) transport activity of estradiol 17-β-glucuronide (E17βG) within the 22 second of microgravity during parabolic flights (33). MRP1 (ABCC1) is a member of the ABCC subfamily, which is structurally almost identical with MDR1 but it can only efflux substrates that conjugates with glutathione (GSH), glucuronate or sulfate compared to MDR1 which has a broader substrate specificity (34, 35). MRP1 (ABCC1) is largely localized at the plasma membrane in Jurkat cells and from a previous study, it was found that multidrug resistance-associated proteins including MRP1 (ABCC1) are responsible for glutathione release especially in cells undergoing apoptosis (36, 37). The study also showed that Jurkat cells released approximately 75-80% of their intracellular GSH for

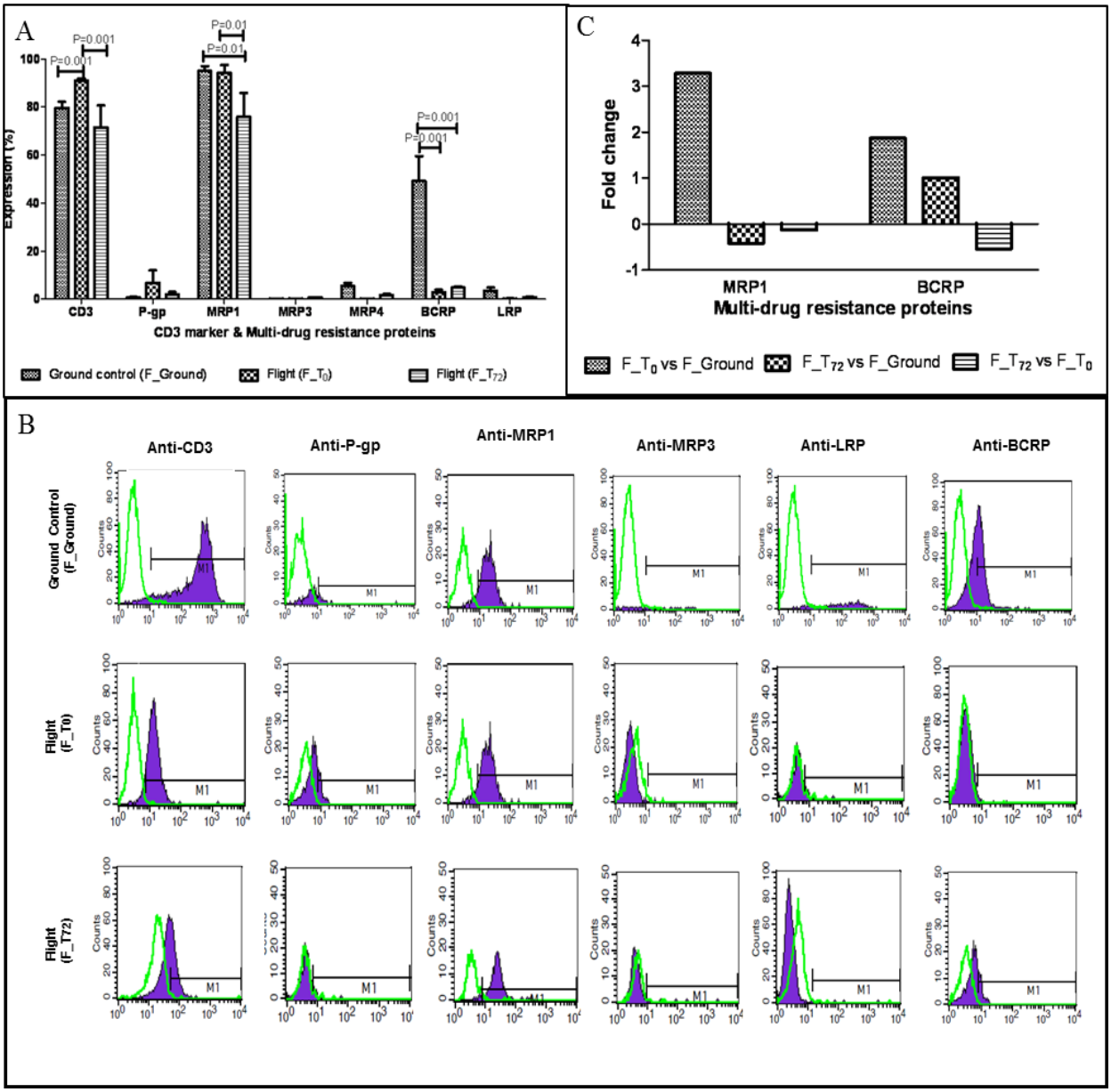

Figure 5. (A) CD3 marker and MDR proteins (P-gp, MRP1, MRP3, MRP4, BCRP and LRP) expression in Jurkat cells at different time point: F_Ground, F_T0 and F_T72. The cells were labeled as described under Materials & Methods. The CD3 marker and MDR expression were determined using flowcytometry. Error bars represent the SEM of triplicates for each sample. Only 3 markers showed significant changes in their expression which are CD3 markers, MRP1 and BCRP proteins while the other proteins did not show significant changes. CD3 markers expression was increased at F_T0 when compared to ground control (F_Ground) and F_T72 with $p<0.001$. As for MRP1 protein, the expression was increased at F_T0 compared to Flight T72 with $p<0.01$ and BCRP protein expression was increased at F_Ground compared to F_T0 and F_T72. (B) Representative of the flowcytometry analysis for CD3 marker and MDR proteins (P-gp, MRP1, MRP3, MRP4, BCRP and LRP) expression in Jurkat cells at different time point: F_Ground, F_T0 and F_T72. The cells were labeled as described under Materials & Methods. Data shown are the histogram plot of the expression markers based on the cell count (Y-axis), and mean fluorescent intensity of the cell expression (X-axis). As predicted, CD3 marker was highly expressed, followed by MRP1 protein in all three time points. BCRP protein was highly expressed in F_Ground sample only, while the other proteins did not show significant changes in expression level. (C) mRNA expression level of MRP1 and BCRP as assessed by RT-PCR assay. A ten-fold dilution series of cDNA (F_Ground) was generated to determine the amplification efficiency of each primer pair. The threshold crossing (Ct) value for each reaction was determined and the fold-change ($\Delta\Delta$Ct value) was calculated using GAPDH as a reference control. As shown in the result, MRP1 mRNA expression was up-regulated at F_T0 compared to ground (F_Ground). But the expressions were down-regulated at time F_T72 when compared to F_T0 and F_Ground indicate that after 72 hours of exposure to microgravity condition the expressions were decreased. Meanwhile, the mRNA expressions of BCRP were up-regulated at both time point, which were F_T0 and F_T72 at microgravity condition compared to ground condition, F_Ground. But when the mRNA expression of BCRP was compared between Flight_T72 and Flight_T0, the expression was down-regulated.

both Fas antibody and staurosporine-induced apoptosis (36). Meanwhile, Lewis et al. (1998) (14) reported that the apoptosis-related factor Fas/APO-1 increased in the culture medium of the space-flown cells and the number of cells with DNA condensation characteristic of apoptosis was increased in flown cells early in the experiment. Thus, reduced expression of MRP1 (ABCC1) and BCRP (ABCG2) in microgravity might be a mechanism of adaptation to support Jurkat cell survival and proliferation in microgravity. As MRP1 (ABCC1) and BCRP (ABCG2) as active transporter proteins that utilizes ATP, reduced intracellular cellular ATP content in microgravity may also cause reduced MRP1 (ABCC1) and BCRP (ABCG2)expression as shown by Vaquer et al. (2014) (33), which demonstrated that on parabolic simulated microgravity, reduction of MRP2 (ABCC2) activity is via the ATP-dependent transport.

The mRNA expression of MRP1 (ABCC1) and BCRP (ABCG2)

The mRNA expression of the MRP1 (ABCC1) and BCRP (ABCG2) were further analyzed by qRT-PCR assays. As shown in Fig.5 C, after normalisation by GAPDH, the results showed up-regulation of MRP1 (ABCC1) mRNA expression at Flight_T0 compared to F_Ground with a fold change of 3.28. Meanwhile, at Flight_T72 vs F_Ground and F_T72 vs F_T0, the MRP1 (ABCC1) mRNA expression was down-regulated with fold change values of -0.42 and -0.13 respectively. This mRNA expression confirmed the protein expression of MRP1 (ABCC1) from the flowcytometry assay. The qRT-PCR results for BCRP (ABCG2) showed that the mRNA expression were up-regulated with fold change values of 1.87 and 1.01 at F_T0 vs F_Ground and F_T72 vs F_Ground respectively. But when F_T72 was compared to F_T0, mRNA expression of BCRP (ABCG2) was down-regulated with a fold change value of -0.54. However from the flowcytometry assay, the BCRP (ABCG2) protein showed totally different expression which the protein expression were down-regulated at flight condition compared to ground condition. The increased mRNA expression in the presence of low protein expression could be explained by the presence of two opposing regulatory mechanisms for BCRP (ABCG2) as mediated by the MEK-ERK signaling pathway, giving a situation where BCRP (ABCG2) gene was up-regulated at the transcriptional level whilst being degraded at the protein level (38). Another possible explanation is the result of epigenetic silencing of BCRP (ABCG2) gene expression through promoter demethylation and this was shown as a key mechanism for the development of ABCG2-dependent MDR phenotype in Jurkat (39).

Decreased gene expression of the membrane ion channel, Kv1.1

The principle component analysis (PCA) in Figure 6 A and 6 B showed that the samples clustered in a distinct pattern, with the samples grouped according to the treatment condition. From our microarray analysis (Fig. 7), the significant differentially expressed genes were clustered appropriately according to the three time points of pre-launch, activation and termination which were designated as F_Ground, F_T0 and F_T72. The hierarchical clustering showed that at F_T0 compared to F_Ground, there were 237 genes that were up-regulated while 362 genes that were down-regulated; as for F_T72 compared to F_Ground, there were 480 genes that were up-regulated while 491 genes that were down-regulated; while for F_T72 compared to FT0, there were 450 genes that were up-regulated while 326 genes that were down-regulated. From the GSEA analysis, the gene set associated with cell membrane was the most affected in all conditions and showed statistical significance in the following conditions: F_T0 compared to F_Ground, F_T72 compared to F_Ground and when F_T72 compared to F_T0 as shown in Table 1. The GSEA analysis provided some key clues as to the cellular changes occurred during the experiment. The membrane-related genes were the only significantly enriched gene set for the launching and docking period (F_T0 vs F_Ground), which suggested that events within this time period affected the expression of genes related to cellular membrane and membrane transporter, and this was further shown in the active MDR protein expression as stated above. Comparison of F_T72 vs F_T0 and F_T72 vs F_Ground revealed gene sets which may indicate adaptation to changes to the gravitational force during spaceflight, and were related to gravisensing such as olfactory receptor activity, G-protein coupled receptor protein signaling pathway, sensory perception to smell and response to stimulus. It was suggested that transmembrane proteins such as ABC transporters and solute carriers play important roles in “sensing” fluctuations or transient changes in the chemical/biochemical composition of the local environment, suggesting that these transporters may also be involve in cellular signaling of graviperception (40), and is postulated to be more pronounced in microgravity conditions (41). Another environmental factor to be considered during spaceflight is space radiation, and previous studies have indicated that space radiation induced accumulated chromosome aberration (42). However, how space radiation might affect transmembrane proteins such as transporter protein and ion channel remains to be elucidated.

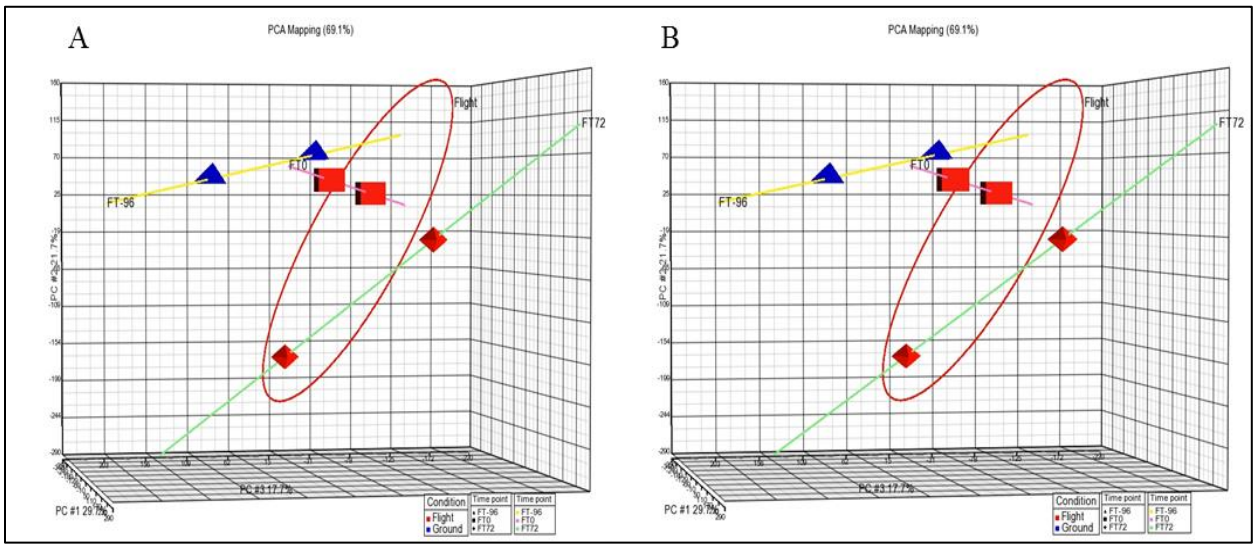

Figure 6. Principal components analysis (PCA) were performed for all the samples according to the expression levels of all probe sets and were represented in three dimensional format. (A) All probe sets were grouped according to conditions, which were flight and ground; (B) All probe sets were grouped according to time and conditions which were Flight_Ground, Flight_T0 and Flight_T72. Each dot represents a chip, the colors represent the condition and the samples were grouped by condition in this figure.

The complete list of differentially expressed genes related to membrane transporters, solute carrier proteins, ion channels, ATP-related kinases, G-coupled protein receptors and membrane structure is shown in Table 2 A, 2 B and 2 C. From the gene expression analysis data, the expression of voltage-gated K+ channel, shaker-related subfamily, member 1 (episodic ataxia with myokymia) (KCNA1), also known as Kv1.1 was found to be significantly down-regulated at F_T72 compared to F_T0 (fold change -1.26, p value < 0.05) while the expression was up-regulated at F_T0 compared to F_Ground (fold change 1.22, p value < 0.05, shown is Table 2 A) and this was confirmed with subsequent qPCR as shown in Fig. 8. The figure also showed that the mRNA expression of KCNA1 was down-regulated at F_T72 compared to F_T0 with fold change of -0.700 while the expression was up-regulated at F_T0 compared to F_Ground with fold change of 3.17. As previous study has demonstrated reduced K+ influx in type II hair cells exposed to simulated microgravity conditions (43), we want to highlight that significant reduced expression of Kv1.1 in spaceflight conditions from our study might shed some light in understanding reduction of K+ current in cells conditioned with microgravity. It has been suggested that microgravity causes the redistribution of transmural pressure within cells, as demonstrated in vascular smooth muscle cells (VSMCs) which showed the differential activation of K+ and Ca2+ channels as part of the vascular adaptation to microgravity (13, 44). In simulated microgravity conditions, the K+ current is smaller in the VSMCs of mice subjected to microgravity compared to control mice (13, 45), while another study showed that there is inactivation of the membrane's Na+ and K+-pumps in mice subjected to hypogravity (between 0 to 1g) (46). Thus, from our study we suggested that the transmembrane proteins has an integral mechanism in gravi-perception and adaptation to gravity changes which previously was only shown in E. coli (9).

There were several limitations to this study. Firstly, due to logistic and time constrain, we are not able to do a simultaneous ground control with the same time point as the flight samples during the spaceflight except for F_Ground. Therefore we have completed the asynchronous ground control study when we returned to Malaysia. However, we found that the results from the asynchronous ground control at T0 were significantly different from F_Ground, thus rendering the asynchronous ground control invalid. We suspected that this is due to the batch of cells that was transported to Baikonur for the spaceflight study has undergo various stress which was not subjected to the same batch of cells from the asynchronous ground control study that remained in the lab back in Malaysia. Therefore the results asynchronous ground control at T0 and T72 were not included here for comparison. The present study also did not capture actual drug / solute transport activity, changes of K+ current and change in transmural pressure during spaceflight to confirm our proposed mechanism due to the limitation of the FPA to do real-time detection.

Table 1. The Gene Set Enrichment Analysis (GSEA) of the different conditions: F_T0 vs F_Ground, F_T72 vs F_Ground, F_T72 vs F_T0.

Conditions	Gene Set Name	Gene Set Category	Genes (red fonts are genes significantly expressed in microarray analysis)	Normalized Enrichment Score	p-value
FT_0 vs F_Ground	Integral to membrane	Cellular component	OR1D2, OR1F1, DNAJC16, OR4F5, OR4F17, OR13C4, GPR111, OR4C12, MS4A10, OR52K1, OR4N2, DGAT1, ADIPOR2, AQP7, SLC31A1, LNPEP, VAMP7, OPN1SW, SLC25A23, SLC25A30	-1.72333	0
	Membrane	Cellular Component	DNAJC16, GPR111, MS4A10, ALOX5, DGAT1, GK, ADIPOR2, AQP7, SLC31A1, GAP43, MLANA, RAB27A, LNPEP, VAMP7, SNF8, GCHFR, OPN1SW, LRRC32, RTN4RL2, SLC25A23, SLC25A30	-1.69245	0.012295
FT_{72} vs F_Ground	G-protein coupled receptor protein signaling pathway	Biological Process	OR1D2, OR1F1, OR4F5, OR4F17, OR13C4, GPR111, OR4C12, OR52K1, OR4N2, OPN1SW	-1.96051	0
	Olfactory receptor activity	Molecular function	OR1D2, OR1F1, OR4F5, OR4F17, OR13C4, OR4C12, OR52K1, OR4N2	-1.90996	0.004082
	Receptor activity	Molecular function	OR1D2, OR1F1, OR4F5, OR4F17, OR13C4, GPR111, OR4C12, MS4A10, OR52K1, OR4N2, ADIPOR2, OPN1SW, RTN4RL2	-1.85696	0.008065
	Response to stimulus	Biological process	OR1D2, OR1F1, OR4F5, OR4F17, OR13C4, OR4C12, OR52K1, OR4N2, OPN1SW	-1.82129	0.00823
	Sensory perception of smell	Biological process	OR1D2, OR1F1, OR4F5, OR4F17, OR13C4, OR4C12, OR52K1, OR4N2	-1.9112	0.008734
	Integral to membrane	Cellular component	OR1D2, OR1F1, DNAJC16, OR4F5, OR4F17, OR13C4, GPR111, OR4C12, MS4A10, OR52K1, OR4N2, DGAT1, ADIPOR2, AQP7, SLC31A1,	-1.82328	0.017857

			LNPEP, VAMP7, OPN1SW, SLC25A23, SLC25A30		
	Plasma membrane	Cellular component	OR1D2, OR1F1, OR4F5, OR4F17, OR13C4, GPR111, OR4C12, OR52K1, OR4N2, CD1A, AQP7, ANXA2, GAP43, PRKACA, LNPEP, RTN4RL2	-1.79134	0.02521
	Nucleic acid binding	Molecular_function	PRDM7, SCRT2, ZNF720, RNASE3, RBM14	-1.70655	0.031818
FT_{72} vs FT_0	Response to stimulus	Biological_process	OR1D2, OR1F1, OR4F5, OR4F17, OR13C4, OR4C12, OR52K1, OR4N2, OPN1SW	-2.02461	0
	Sensory perception of smell	Biological_process	OR1D2, OR1F1, OR4F5, OR4F17, OR13C4, OR4C12, OR52K1, OR4N2	-1.94178	0
	G-protein coupled receptor protein signaling pathway	Biological_process	OR1D2, OR1F1, OR4F5, OR4F17, OR13C4, GPR111, OR4C12, OR52K1, OR4N2, OPN1SW	-2.13556	0
	Olfactory receptor activity	Molecular_function	OR1D2, OR1F1, OR4F5, OR4F17, OR13C4, OR4C12, OR52K1, OR4N2	-1.96479	0.005714
	Receptor activity	Molecular_function	OR1D2, OR1F1, OR4F5, OR4F17, OR13C4, GPR111, OR4C12, MS4A10, OR52K1, OR4N2, ADIPOR2, OPN1SW, RTN4RL2	-1.82281	0.006667
	Proteinaceous extracellular matrix	Cellular component	VWA1, ANXA2, WNT6, VWC2, SLC25A23	1.73939	0.008584
	Cytosol	Cellular component	ALOX5, DGAT1, GK, PRKACA, KPNA1, GCHFR, DYNC1I2, PRKAG1	1.567	0.008811
	Detection of chemical stimulus involved in sensory perception of smell	Biological_process	OR1D2, OR1F1, OR13C4, OR4C12, OR52K1, OR4N2	-1.66528	0.024876
	Transferase activity	Molecular_function	PRDM7, DGAT1, GK, PRKACA, PDK2, STK35	1.55745	0.05

Table 2. List of significant differentially expressed genes of Jurkat cells when these conditions were compared: (A) F_T0 vs F_Ground, (B) F_T72 vs F_Ground and (B) F_T72 vs F_T0.

Table 2 A (F_T_0 vs F_Ground)

Gene Symbol	Gene Description	p-value	Fold-Change
Solute carrier protein			
SLC35B1	solute carrier family 35, member B1	0.002076	-1.22313
SLC31A1	solute carrier family 31 (copper transporters), member 1	0.004083	-1.48776
SLC34A2	solute carrier family 34 (sodium phosphate), member 2	0.004842	-1.14291
SLC2A12	solute carrier family 2 (facilitated glucose transporter), member 12	0.006507	1.10632
SLC37A4	solute carrier family 37 (glucose-6-phosphate transporter), member 4	0.008433	-1.25573
SLC5A2	solute carrier family 5 (sodium/glucose cotransporter), member 2	0.009854	-1.15297
SLC6A8	solute carrier family 6 (neurotransmitter transporter, creatine), member 8	0.009883	1.10204
SLC25A23	solute carrier family 25 (mitochondrial carrier; phosphate carrier), member 23	0.01122	-1.39962
SLC38A3	solute carrier family 38, member 3	0.017454	-1.12192
SLC25A30	solute carrier family 25, member 30	0.035208	-1.35439
SLC4A1	solute carrier family 4, anion exchanger, member 1 (erythrocyte membrane protein band 3, Diego blood group)	0.048194	-1.22052
SLC32A1	solute carrier family 32 (GABA vesicular transporter), member 1	0.048946	1.15127
Ion Channel			
KCTD8	potassium channel tetramerisation domain containing 8	0.003586	1.16205
KCTD1	potassium channel tetramerisation domain containing 1	0.003811	-1.15467
KCTD20	potassium channel tetramerisation domain containing 20	0.005015	-1.28925
ABCC10	ATP-binding cassette, sub-family C (CFTR/MRP), member 10	0.005728	-1.20341
KCNA2	potassium voltage-gated channel, shaker-related subfamily, member 2	0.017043	1.16571

P2RX6	purinergic receptor P2X, ligand-gated ion channel, 6	0.027085	-1.21747
KCNA1	potassium voltage-gated channel, shaker-related subfamily, member 1 (episodic ataxia with myokymia)	0.0379696	1.22194
SCN7A	sodium channel, voltage-gated, type VII, alpha	0.034705	1.18351
KCTD19	potassium channel tetramerisation domain containing 19	0.037211	1.2067
SCLT1	sodium channel and clathrin linker 1	0.038636	1.41658
SCN1B	sodium channel, voltage-gated, type I, beta	0.042473	-1.22595
ABCC4	ATP-binding cassette, sub-family C (CFTR/MRP), member 4	0.042018	1.11811
CIB3	calcium and integrin binding family member 3	0.045032	-1.43152
ATP-related kinase			
CLPP	ClpP caseinolytic peptidase, ATP-dependent, proteolytic subunit homolog (E. coli)	0.007669	1.23721
ARHGAP19	Rho GTPase activating protein 19	0.008502	-1.34514
PRKAR2B	protein kinase, cAMP-dependent, regulatory, type II, beta	0.009811	1.166
PRKAG1	protein kinase, AMP-activated, gamma 1 non-catalytic subunit	0.012086	-1.47962
PRKAG2	protein kinase, AMP-activated, gamma 2 non-catalytic subunit	0.019335	1.15804
ATP9A	ATPase, class II, type 9A	0.021946	-1.17968
RAB3GAP1	RAB3 GTPase activating protein subunit 1 (catalytic)	0.033157	-1.13793
ATPAF2	ATP synthase mitochondrial F1 complex assembly factor 2	0.036344	-1.22903
AGBL3	ATP/GTP binding protein-like 3	0.04537	1.21659
G-protein coupled receptors			
RGS16	regulator of G-protein signaling 16	0.008423	1.22155
GPR123	G protein-coupled receptor 123	0.013766	-1.13188
GPR125	G protein-coupled receptor 125	0.043781	-1.83386
GPR126	G protein-coupled receptor 126	0.045163	-1.17472

Membrane related			
VTI1A	vesicle transport through interaction with t-SNAREs homolog 1A (yeast)	0.001821	1.2103
VAMP7	vesicle-associated membrane protein 7	0.002499	-1.37737
TMEM51	Transmembrane protein 51	0.00324	1.18029
MS4A10	membrane-spanning 4-domains, subfamily A, member 10	0.005354	-1.35679
VPS37A	vacuolar protein sorting 37 homolog A (S. cerevisiae)	0.005493	1.3781
TOMM7	translocase of outer mitochondrial membrane 7 homolog (yeast)	0.008786	1.41451
TMEM104	Transmembrane protein 104	0.010172	-1.45768
TMEM101	Transmembrane protein 101	0.01191	-1.19942
TMEM154	Transmembrane protein 154	0.014112	1.10695
TAPT1	transmembrane anterior posterior transformation 1	0.014327	1.17844
TMEM20	Transmembrane protein 20	0.016412	1.13919
TMEM181	Transmembrane protein 181	0.017986	1.20304
TMUB2	transmembrane and ubiquitin-like domain containing 2	0.020331	-1.13685
TMEM225	Transmembrane protein 225	0.026755	1.13499
TMEM54	Transmembrane protein 54	0.031018	1.14666
TMPRSS11E	transmembrane protease, serine 11E	0.041309	-1.164
MS4A2	membrane-spanning 4-domains, subfamily A, member 2 (Fc fragment of IgE, high affinity I, receptor for; beta	0.046502	-1.20104
VSTM2L	V-set and transmembrane domain containing 2 like	0.047961	-1.11588
TMEM55A	Transmembrane protein 55A	0.048228	-1.21082
LRBA	LPS-responsive vesicle trafficking, beach and anchor containing	0.049176	1.12082

Table 2 (A) *Continued*

Table 2 B (F_T_{72} vs F_Ground)

Gene Symbol	Gene Description	p-value	Fold-Change
Solute carrier protein			
SLC43A1	solute carrier family 4, anion exchanger, member 2 (erythrocyte membrane protein band 3-like 1)	0.000483668	1.16667

SLC35B1	solute carrier family 35, member B1	0.001212	-1.27362
SLC31A1	solute carrier family 31 (copper transporters), member 1	0.011173	-1.32172
SLC25A30	solute carrier family 25, member 30	0.012717	-1.55885
SLC4A2	solute carrier family 4, anion exchanger, member 2 (erythrocyte membrane protein band 3-like 1)	0.013438	1.15435
SLC27A6	solute carrier family 27 (fatty acid transporter), member 6	0.017446	-1.16772
SLC26A3	solute carrier family 26, member 3	0.017951	-1.34739
SLC25A33	solute carrier family 25, member 33	0.023815	1.39022
SLC25A23	solute carrier family 25, member 23	0.030528	-1.26126
SLC35E2	solute carrier family 35, member E2	0.031297	1.11007
SLC35D3	solute carrier family 35, member D3	0.0399	1.17568
SLC17A4	solute carrier family 17 (sodium phosphate), member 4	0.045745	-1.14266
SLC7A4	solute carrier family 7 (cationic amino acid transporter, y+ system), member 4	0.046064	1.19786
SLC10A6	solute carrier family 10 (sodium/bile acid cotransporter family), member 6	0.0462567	-1.40165
SLC5A1	solute carrier family 5 (sodium/glucose cotransporter), member 1	0.0471076	1.20599
SLC35F1	solute carrier family 35, member F1	0.0499886	1.23828
Ion channel			
KCTD8	potassium channel tetramerisation domain containing 8	0.001463	1.22639
KCNA2	potassium voltage-gated channel, shaker-related subfamily, member 2	0.004775	1.27261
P2RX2	purinergic receptor P2X, ligand-gated ion channel, 2	0.008085	1.19353
KCTD20	potassium channel tetramerisation domain containing 20	0.010361	-1.2175
NHEDC2	Na+/H+ exchanger domain containing 2	0.012598	1.10283
CACNA2D2	calcium channel, voltage-dependent, alpha 2/delta subunit 2	0.022713	1.21665
EFCAB2	EF-hand calcium binding domain 2	0.027752	1.34066

SCNN1G	sodium channel, nonvoltage-gated 1 gamma	0.028029	1.10861
TRPV2	transient receptor potential cation channel, subfamily V, member 2	0.028363	1.24184
P2RX4	purinergic receptor P2X, ligand-gated ion channel, 4	0.0293057	1.29668
C2CD4C	C2 calcium-dependent domain containing 4C	0.035394	1.43904
SCN4B	sodium channel, voltage-gated, type IV, beta	0.035977	1.18436
KCTD3	potassium channel tetramerisation domain containing 3	0.037413	-1.14608
HVCN1	hydrogen voltage-gated channel 1	0.040963	-1.16463
KCTD18	potassium channel tetramerisation domain containing 18	0.044126	-1.10755
KCNF1	potassium voltage-gated channel, subfamily F, member 1	0.048869	1.18261

ATP-related kinase

GCHFR	GTP cyclohydrolase I feedback regulator	0.001879	1.45611
AKAP14	A kinase (PRKA) anchor protein 14	0.003829	-1.40096
ARHGAP19	Rho GTPase activating protein 32	0.003993	-1.47126
GTPBP8	GTP-binding protein 8 (putative)	0.005972	1.39796
ATP1A4	ATPase, Na+/K+ transporting, alpha 4 polypeptide	0.010485	-1.12353
ATP7A	ATPase, Cu++ transporting, alpha polypeptide	0.011789	-1.16944
ARHGAP32	Rho GTPase activating protein 32	0.012454	-1.2471
ATP6V1B2	ATPase, H+ transporting, lysosomal 56/58kDa, V1 subunit B2	0.013912	-1.19647
ATP6V0A2	ATPase, H+ transporting, lysosomal V0 subunit a2	0.022099	-1.17263
RAB3GAP1	RAB3 GTPase activating protein subunit 1 (catalytic)	0.023323	-1.15927
PDP1	protein phosphatase 2C, magnesium dependent, catalytic subunit	0.025084	-1.26558
ATP6V1G3	ATPase, H+ transporting, lysosomal 13kDa, V1 subunit G3	0.036408	-1.20651
PRKD3	protein kinase D3	0.039796	-1.21945

ARHGAP29	Rho GTPase activating protein 29	0.040009	-1.12884
TPTE2	transmembrane phosphoinositide 3-phosphatase and tensin homolog 2	0.041466	-1.765
AAK1	AP2 associated kinase 1	0.049479	1.28673
G-protein coupled receptors			
RGSL1	regulator of G-protein signaling like 1	0.002762	-1.20137
GPR111	G protein-coupled receptor 111	0.014733	-1.80449
GPR107	G protein-coupled receptor 107	0.025884	-1.22082
S1PR1	endothelial differentiation, sphingolipid G-protein-coupled receptor, 1	0.029012	1.12094
GRK1	G protein-coupled receptor kinase 1	0.033318	1.40565
GPR146	G protein-coupled receptor 146	0.040085	-1.24499
P2RY13	purinergic receptor P2Y, G-protein coupled, 13	0.040725	-1.17363
GPR12	G protein-coupled receptor 12	0.047687	1.49763
Membrane related			
MS4A10	membrane-spanning 4-domains, subfamily A, member 10	0.00118	-1.66906
VAMP7	vesicle-associated membrane protein 7	0.001656	-1.44545
TMEM169	transmembrane protein 169	0.00415673	-1.13496
TAPT1	transmembrane anterior posterior transformation 1	0.00792	1.22504
GPNMB	glycoprotein (transmembrane) nmb	0.009405	-1.28609
TMEM192	transmembrane protein 192	0.013005	-1.19482
TMEM42	transmembrane protein 42	0.015334	1.67896
TMEM55A	transmembrane protein 55A	0.0154914	-1.34376
TMEM194B	transmembrane protein 194B	0.0180827	1.1965
TMEM155	transmembrane protein 155	0.018505	-1.25386
TMEM63B	transmembrane protein 63B	0.021784	-1.10553
TMEM151A	transmembrane protein 151A	0.028522	1.29596
TMEM30A	transmembrane protein 30A	0.028629	-1.32616
TMEM54	transmembrane protein 54	0.042299	1.12881
TMEM86A	transmembrane protein 86A	0.042955	-1.15306
TMCO1	transmembrane and coiled-coil domains 1	0.045392	1.48957

TMPRSS3	transmembrane protease, serine 3	0.045832	1.149
TMEM22	transmembrane protein 22	0.047858	1.18997
TMEM184C	transmembrane protein 184C	0.049762	-1.35063

Table 2 C (F_T_{72} vs F_T_0)

Gene Symbol	Gene Description	p-value	Fold-Change
Solute carrier protein			
SLC43A1	solute carrier family 43, member 1	0.000680992	1.14727
SLC39A9	solute carrier family 39 (zinc transporter), member 9	0.00185424	-1.13771
SLC5A2	solute carrier family 5 (sodium/glucose cotransporter), member 2	0.0077808	1.16739
SLC34A2	solute carrier family 34 (sodium phosphate), member 2	0.0104302	1.10735
SLC38A3	solute carrier family 38, member 3	0.0135695	1.1344
SLC4A2	solute carrier family 4, anion exchanger, member 2 (erythrocyte membrane protein band 3-like 1)	0.0151569	1.14728
SLC2A11	solute carrier family 2 (facilitated glucose transporter), member 11	0.0165409	1.21121
SLC35D3	solute carrier family 35, member D3	0.0204992	1.23236
SLC19A2	solute carrier family 19 (thiamine transporter), member 2	0.0271786	-1.18018
SLC15A3	solute carrier family 15, member 3	0.0299038	1.2753
SLC25A33	solute carrier family 25, member 33	0.0328524	1.33824
SLC46A1	solute carrier family 46 (folate transporter), member 1	0.0384373	1.48451
SLC1A7	solute carrier family 1 (glutamate transporter), member 7	0.0433297	1.2078
SLC22A18	solute carrier family 22, member 18	0.0469688	1.14635
SLC25A42	solute carrier family 25, member 42	0.0470548	1.10678
SLCO2A1	solute carrier organic anion transporter family, member 2A1	0.0491312	1.31316
Ion Channel			

ATP1A4	ATPase, Na+/K+ transporting, alpha 4 polypeptide	0.00623656	-1.15021
KCTD18	potassium channel tetramerisation domain containing 18	0.00785901	-1.21423
NHEDC2	Na+/H+ exchanger domain containing 2	0.00855772	1.11894
P2RX2	purinergic receptor P2X, ligand-gated ion channel, 2	0.0123095	1.16449
PIRT	phosphoinositide-interacting regulator of transient receptor potential channels	0.0199073	1.42512
NKAIN4	Na+/K+ transporting ATPase interacting 4	0.0204165	1.22028
SCN7A	sodium channel, voltage-gated, type VII, alpha	0.0278392	-1.20135
ABCC4	ATP-binding cassette, sub-family C (CFTR/MRP), member 4	0.0306134	-1.13474
ABCE1	ATP-binding cassette, sub-family E (OABP), member 1	0.0323689	1.10822
SCNN1G	sodium channel, nonvoltage-gated 1, gamma	0.0342303	1.10016
CACNA2D2	calcium channel, voltage-dependent, alpha 2/delta subunit 2	0.0365717	1.17747
KCNA1	potassium voltage-gated channel, shaker-related subfamily, member 1 (episodic ataxia with myokymia)	0.0379696	-1.26194
KCNK6	potassium channel, subfamily K, member 6	0.0400672	1.33111
P2RX6	purinergic receptor P2X, ligand-gated ion channel, 6	0.0491017	1.16849
CACNA1F	calcium channel, voltage-dependent, L type, alpha 1F subunit	0.0495933	1.22065
ATP-related kinase			
GCHFR	GTP cyclohydrolase I feedback regulator	0.00460838	1.31802
PRKACA	protein kinase, cAMP-dependent, catalytic, alpha	0.00564514	1.38474
ATP1A4	ATPase, Na+/K+ transporting, alpha 4 polypeptide	0.00623656	-1.15021
ARHGAP29	Rho GTPase activating protein 29	0.0088749	-1.2363
HIPK1	homeodomain interacting protein kinase 1	0.0142931	-1.27039
AGAP3	ArfGAP with GTPase domain, ankyrin repeat and PH domain 3	0.0155017	1.14692
ATP9A	ATPase, class II, type 9A	0.0165343	1.20141
ATP6V1G3	ATPase, H+ transporting, lysosomal 13kDa, V1 subunit G3	0.0166057	-1.28742

PIRT	phosphoinositide-interacting regulator of transient receptor potential channels	0.0199073	1.42512
ATP6V1B2	ATPase, H+ transporting, lysosomal 56/58kDa, V1 subunit B2	**0.023509**	**-1.1593**
ARHGAP32	Rho GTPase activating protein 32	0.0275971	-1.17883
GTPBP8	GTP-binding protein 8 (putative)	0.0287369	1.20853
PRKAR2B	protein kinase, cAMP-dependent, regulatory, type II, beta	0.0312998	-1.10528
MAGI3	membrane associated guanylate kinase, WW and PDZ domain containing 3	0.0366259	-1.22959
ATP6V0A2	ATPase, H+ transporting, lysosomal V0 subunit a2	0.0374475	-1.13894
ATP6V0E2	ATPase, H+ transporting V0 subunit e2	0.0458932	1.20556
PPP1R16A	protein phosphatase 1, regulatory (inhibitor) subunit 16A	0.0473538	1.1437
ROR1	receptor tyrosine kinase-like orphan receptor 1	0.0476281	1.17361
G- protein coupled receptors			
GPR88	G protein-coupled receptor 88	0.00675097	1.14835
RGS16	regulator of G-protein signaling 16	0.00730777	-1.23418
RGSL1	regulator of G-protein signaling like 1	0.00753746	-1.13825
P2RY14	purinergic receptor P2Y, G-protein coupled, 14	0.0205441	-1.21992
GPR123	G protein-coupled receptor 123	0.0245975	1.10514
P2RY13	purinergic receptor P2Y, G-protein coupled, 13	0.0398972	-1.17517
Membrane related			
VTI1A	vesicle transport through interaction with t-SNAREs homolog 1A (yeast)	0.000632303	-1.31397
VPS72	vacuolar protein sorting 72 homolog (S. cerevisiae)	0.00669886	1.20825
REEP4	receptor accessory protein 4	0.00694598	1.23343
TMEM154	transmembrane protein 154	0.0112493	-1.11658
TMEM129	transmembrane protein 129	0.0142851	1.11112
ELTD1	EGF, latrophilin and seven transmembrane domain containing 1	0.0147176	-1.12582

MS4A10	membrane-spanning 4-domains, subfamily A, member 10	0.0159023	-1.23015
TMEM182	transmembrane protein 182	0.0159559	-1.33732
VSTM2L	V-set and transmembrane domain containing 2 like	0.0205864	1.16435
TMEM151A	transmembrane protein 151A	0.0231532	1.3239
TMEM120B	transmembrane protein 120B	0.0277194	-1.9532
TMEM63A	transmembrane protein 63A	0.0297914	1.15965
TMEM192	transmembrane protein 192	0.0315646	-1.13647
TMEM101	transmembrane protein 101	0.0356456	1.12836
TMEM42	transmembrane protein 42	0.0367047	1.45179
TMEM225	transmembrane protein 225	0.041941	-1.11215
TMEM194B	transmembrane protein 194B	0.0458763	1.36888
TMEM209	transmembrane protein 209	0.0462972	-1.12745
TMEM161B	transmembrane protein 161B	0.0481367	-1.25183
TMCO3	transmembrane and coiled-coil domains 3	0.0492635	1.11171

However, the results gleamed from the present study warrant further investigation on real-time drug transport activity and ion channel activity in simulated microgravity and during spaceflight. Due to limited samples, we are also unable to do further downstream studies to confirm our observation, such as changes of PKC levels and changes at the Kv1.1 channels; however, the current observations might serve as a basis for a follow-up study with more comprehensive experimental parameters to be conducted under simulated microgravity conditions.

One of the practical implications of the present study is a better understanding of pharmacodynamics of drugs during spaceflight, especially for long term spaceflight, whereby astronaut may need drug administration during medical emergencies (2). Currently, there is insufficient information regarding effects of drugs in space (47, 48), especially on the effects of weightlessness on drug transporters and its activity. To our knowledge, the present study is among the first to evaluate how spaceflight and microgravity could affect the various MDR transporter proteins in vitro in a stable microgravity platform. Reduced transmembrane drug transporter capabilities during spaceflight may lead to slower drug clearance, leading to drug accumulation and toxic effect (33). However, overexpression of these proteins may lead to drug resistance in cancer treatment (49, 50). Further investigation derived from the present findings could help elucidate the mechanism of action of the transmembrane drug transporters and provide new information for development of better drugs in the future.

In conclusion, we found that spaceflight affected the expression of membrane transporter proteins such as MRP1 and BRCP which are related to multidrug resistance as well as voltage-gated K+ channel (Kv1.1). The findings suggested

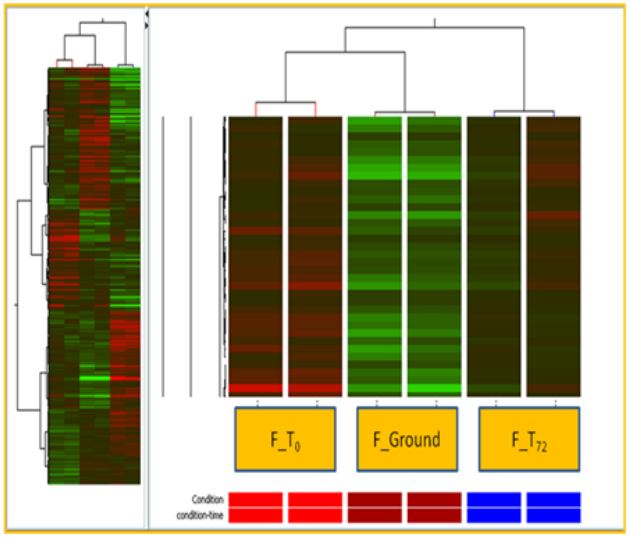

Figure 7. Hierachical clustering of the differentially expressed genes of F_Ground, F_T0 and F_T72 with p-value ≤ 0.05, fold change ≥ ± 1.2. Each row represents a single transcript and each column an experimental sample. Red and green colours correspond to up- and down-regulation, respectively, with a darker colour denoting less differential expression. Transcripts were hierarchically clustered into those with similar profiles, which were showed to cluster according to experimental conditions.

that altered expression of these transmembrane proteins played a role in cellular perception and adaptation to gravitational changes and microgravity during spaceflight. Although a previous study reported the voltage-gated ion channel porin to be affected by microgravity (9) and

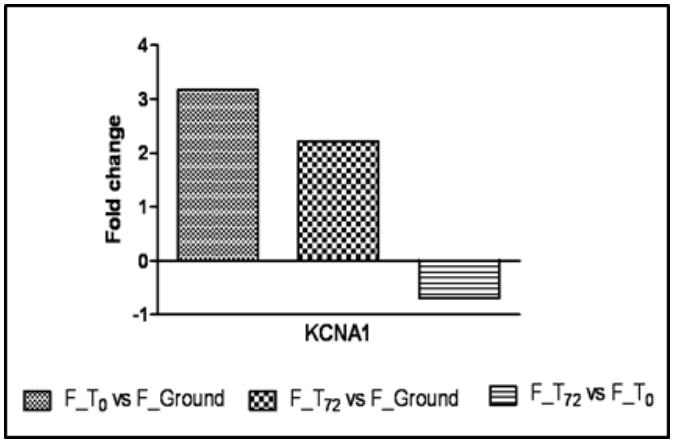

Figure 8. The mRNA expression level of KCNA1 gene as assessed by RT-PCR assay. Briefly, quantification of mRNA expression level were briefly descript in Fig 4 (b) legand. The expression of KCNA1 mRNA transcript was higher in both F_T0 and F_T72 compared to F_Ground while the mRNA expression were down-regulated in F_T72 compared to F_T0. This RT-PCR result validated the microarray analysis.

reduction of MRP2 transport activity in Sf9 insert cells under microgravity condition created by parabolic flight (8), our study examined a wider range of membrane transporters and found that MRP1, BCRP and KCNA1 (Kv1.1) in mammalian cells were significantly affected at different time points during spaceflight. Spaceflight exposed cells to stressful changes at the physical microevironment level, understanding the changes induced at the cellular membrane, including transporter proteins and ion channel may shed important information regarding how cells perceive or "sense" modulation of gravitational force. Cellular and structural changes during spaceflight will affect the pharmacodynamics and pharmacokinetics in the human body, as the increase demand to bring more medication to space will requires scientist and doctors to better understand how our bodies will respond to drug while in space.

Acknowledgements

We would like to thank all staff of the, Institute for Biomedical Problems (IBMP) (Moscow, Russia) and the Russian Federal Space Agency (ROSCOSMOS) for the invaluable assistance during the preparation of the spaceflight samples. This study was funded by the Ministry of Science, Technology and Innovation Malaysia under the grant UKM-ANGKASA-NBD-0018-2007 grant.

Disclosure Statement

The authors declare that they have no competing interests.

References

1. Billica RD, Simmons SC, Mathes KL, McKinley BA, Chuang CC, Wear ML, et al. Perception of the medical risk of spaceflight. . Aviat Space Environ Med 1996;67()(5):467–73.
2. Eyal S, Derendorf H. Medications in Space: In Search of a Pharmacologist's Guide to the Galaxy. Pharm Res. 2019;36(10):148.
3. Jones PM, Goerge AM. The ABC transporter structure and mechanism: prespectives on recent research. Cellular and Molecular Life Sciences. 2004;61:682 - 99.
4. Krishnamurthy P, Schuetz JD. The ABC transporter Abcg2/Bcrp: Role in hypoxia mediated survival. BioMetals. 2005;18:349 - 58.
5. Fazlina N, Maha A, Jamal R, Zarina AL, Cheong SK, Hamidah A, et al. Expression of multidrug resistance (MDR) proteins and in vitro drug resistance in acute leukemias. Hematology. 2007;12:33-7.
6. Amaral L, Engi H, Viveiros M, Molnar J. Review. Comparison of multidrug resistant efflux pumps of cancer and bacterial cells with respect to the same inhibitory agents. In Vivo. 2007;21(2):237-44.
7. Zhang Y, Lu T, Wong M, Wang X, Stodieck L, Karouia F, et al. Transient gene and microRNA expression profile changes of confluent human fibroblast cells in spaceflight. FASEB J. 2016;30(6):2211-24.
8. Vaquer S, Cuyàs E, Rabadán A, González A, Fenollosa F, de la Torre R. Active transmembrane drug transport in microgravity: a validation study using an ABC transporter model. F1000Res. 2014;3:201.
9. Goldermann M, Hanke W. Ion channel are sensitive to gravity changes. Microgravity Sci Technol. 2001;13:35-8.
10. Lu SK, Bai S, Javeri K, Brunner LJ. Altered cytochrome P450 and P-glycoprotein levels in rats during simulated weightlessness. Aviat Space Environ Med. 2002;73(2):112–8.
11. Wilson JW, Ott CM, Höner zu Bentrup K, Ramamurthy R, Quick L, Porwollik S, et al. Space flight alters bacterial gene expression and virulence and reveals a role for global regulator Hfq. Proc Natl Acad Sci U S A. 2007;104(41):16299–304.
12. Crabbé A, Nielsen-Preiss SM, Woolley CM, Barrila J, Buchanan K, McCracken J, et al. Spaceflight enhances cell aggregation and random budding in Candida albicans. PLoS One. 2013;8(12):e80677.
13. Fu ZJ, Xie MJ, Zhang LF, Cheng HW, Ma J. Differential activivation of potassium channels in cerebral and hindquarter arteries of rats during simulated microgravity. Am J Physiol Heart Circ Physiol. 2004;287:1505-15.
14. Lewis ML, Reynolds JL, Cubano LA, Hatton JP, Lawless BD, and Piepmeier EH. Spaceflight alters microtubules and increases apoptosis in human lymphocytes (Jurkat). The FASEB Journal. 1998;12:1007 - 18.
15. Lewis ML, Cubano LA, Baiteng Z, Hong-Khanh D, Pabalan JG, Piepmeier EH, et al. cDNA microarray reveals altered cytoskeleton gene expression in space-flown leukemic T lymphocytes (Jurkat). The FASEB Journal. 2001.

16. Cubano LA, Lewis ML. Fas/APO-1 protein is increased in spaceflown lymphocytes (Jurkat). Experimental Gerontology. 2000;35:389-400.
17. Gasperi V, Rapino C, Battista N, Bari M, Mastrangelo N, Angeletti S, et al. A functional interplay between 5-lipoxygenase and μ-calpain affects survival and cytokine profile of human Jurkat T lymphocyte exposed to simulated microgravity. Biomed Res Int. 2014:782390.
18. Tipton C, Greenleaf J, Jackson C. Neuroendocrine and immune system responses with spaceflights. Medicine & Science in Sports & Exercise 1996;28:988-98.
19. Schmitt DA, Hatton JP, Emond C, Chaput D, Paris H, Levade T, et al. The distribution of protein kinase C in human leukocytes is altered in microgravity. FASEB Journal. 1996;10:1627 - 34.
20. Schatten H, Lewis ML, Chakrabarti A. Spaceflight and clinorotation cause cytoskeleton and mitochondria changes and increases in apoptosis in cultured cells. Acta Astronautica. 2001;49:399-418.
21. Degan P, Sancandi M, Zunino A, Ottaggio L, Viaggi S, Cesarone F, et al. Exposure of human lymphocytes and lymphoblastoid cells to simulated microgravity strongly affects energy metabolism and DNA repair. J Cell Biochem. 2005;94:460-9.
22. Hilaire E, Brown CS, Guikema JA. The Fluid Processing Apparatus: From flight hardware to electron micrographs. J Gravit Physiol. 1995;2:P165-6.
23. Livak KJ, Schmittgen TD. Analysis of relative gene expression data using real-time quantitative PCR and the 2-ΔΔCt method. Methods. 2001;25:402-8.
24. Rozen S, Skaletsky H. Primer3 on the WWW for general users and for biologist programmers. Methods Molecular Biology. 2000;132:365-86.
25. Hunt L, Hacker DL, Grosjean F, De Jesus M, Uebersax L, Jordan M, et al. Low-temperature pausing of cultivated mammalian cells. Biotechnol Bioeng. 2005;89(2):157-63.
26. Franke J, Abs V, Zizzadoro C, Abraham G. Comparative study of the effects of fetal bovine serum versus horse serum on growth and differentiation of primary equine bronchial fibroblasts. BMC Vet Res. 2014;10:119.
27. Singh K, CUbano LA, Lewis ML. Effects of gravitational pertubation on the expression of gens regulating metabolism in Jurkat cells. Bol Assoc Med P R. 2010;102(3):21-6.
28. Weiss A, Imboden J, Hardy K, Manger B, Terhorst C, Stobo J. The role of the T3/antigen receptor complex in T-cell activation. Annu Rev Immunol. 1986;4:593-619.
29. de Groot RP, Rijken PJ, den Hertog J, Boonstra J, Verkleij AJ, de Laat SW, et al. Nuclear responses to protein kinase C signal transduction are sensitive to gravity changes. Exp Cell Res. 1991;197:87-90.
30. Hatton JP, Gaubert F, Lewis ML, Darsel Y, Ohlmann P, Cazenave J-P, et al. The kinetics of translocation and cellular quantity of protein kinase C in human leukocytes are modified during spaceflight. The FASEB Journal. 1999;13:S23 - S33.
31. Matsuda M, Maeda Y, Shirakawa C, Morita, S., Koyama, A., Horiuchi, F., Hamazaki, H., Irimajiri, K. and Horiuchi, A. Possible involvement of protein kinase C activation in down-regulation of CD3 antigen on adult T cell leukaemia cells. British Journal of Haematology. 1994;86:399 -401.
32. Hatton JP, Gaubert F, Lewis ML, Darsel Y, Ohlmann P, Cazenave J-P, et al. The kinetics of translocation and cellular quantity of protein kinase C in human leukocytes are modified during spaceflight. The FASEB Journal. 1999;13:23 - 33.
33. Vaquer S, Cuyàs E, Rabadán A, Gonzalez A, Fenollosa F, de la Torre R. Active transmembrane drug transport in microgravity: a validation study using an ABC transporter model. F1000Res. 2014;3:201.
34. Jedlitschky G, Leier I, Buchholz U, Barnouin K, Kurz G, Keppler D. Transport of glutathione, glucoronate and sulfate conjugates by the MRP gene-encoded conjugate export pump. Cancer Res. 1996;56:988-94.
35. Cole SP, Deeley RG. Multidrug resistance mediated by the APT-binding cassette transporter protein MRP. Bioassays. 1998;20:931-40.
36. Hammond CL, Marchan R, Krance SM, Ballatori N. Glutathione export during apoptosis requires functional multidrug resistance-associated proteins. The Journal of Biological Chemistry. 2007;282(19):14337-47.
37. Marchan R, Hammond CL, Ballatori N. Multidrug resistance-associated protein 1 as a major mediator of basal and apoptotic gluthathione release. Biochim Biophy Acta. 2008;1778:2314-420.
38. Imai Y, Ohmori K, Yasuda S, Wada M, Suzuki T, Fukuda K, et al. Breast cancer resistance protein/ABCG2 is differentially regulated downstream of extracellular signal-regulated kinase. Cancer Science. 2009;6(6):1118-27.
39. Bram EE, Stark M, Raz S, Assaraf YG. Chemotherapeutic drug-induced ABCG2 promoter demethylation as a novel mechanism of acquired multidrug resistance. Neoplasia. 2009;11:1359-70.
40. Wu W, Dnyanmote AV, Nigam SK. Remote communication through solute carriers and ATP binding cassette drug transporter pathways: an update on the remote sensing and signaling hypothesis. Mol Pharmacol. 2011;79:795-805.
41. van Loon JJWA. Mechanomics and physiocomics in gravisensing. Microgravity Sci Technol. 2009;21:159-67.
42. Maalouf M, Durante M, Foray N. Biological effects of space radiation on human cells: History, advances and outcomes. J Radial Res. 2011;52:126-46.
43. Martini M, Canella R, Leparulo A, Prigioni I, Fesce R, Rossi ML. Ionic currents in hair cells dissociated from frog semicircular canals after preconditioning under microgravity conditions. . Am JPhysiolRegul Integr CompPhysiol 2009;296:R1585–R97.
44. Tricarico D, Mele A, Conte Camerino D. Phenotype-dependent functional and pharmacological properties of BKCA channels in skeletal muscle: effects of microgravity. . Neurobiol Dis 2005;20(296–302.).
45. Xie MJ, Ma YG, Gao F, Bai YG, Cheng JH, Chang YM, et al. Activation of BKCa channel is associated with increased apoptosis of cerebrovascular smooth muscle cells in simulated microgravity rats. Am J Physiol Cell Physiol. 2010;298(6):C1489-500.
46. Tyapkina O, Volkov E, Nurullin L, Shenkman B, Kozlovskaya I, Nikolsky E, et al. Resting membrane potential

and Na+, K+-APPase of rat fast and slow muscle during modeling of hypogravity. Physiol Res. 2009;58:599-603.
47. Gandia P, Saivin S, Houin G. The influence of weightlessness on pharmacokinetics. Fundam Clin Pharmacol. 2005;19(6):625–36.
48. Graebe A, Schuck EL, Derendorf H, Lensing P, Putcha L. Physiological, pharmacokinetic and pharmacodynamic changes in space. J Clin Pharmacol. 2004;44(8):837–53.
49. Doyle LA, Ross DD. Multidrug resistance mediated by the breast cancer resistance protein BCRP (ABCG2). Oncogene. 2003;22:7340-58.
50. Kage K, Tsukahara S, Sugiyama T, Asada S, Ishikawa E, Tsuruo T, et al. Dominant-negative inhibition of breast cancer resistance protein as drug efflux pump through the inhibition of S-S dependent homodimerization. Int J Cancer. 2002;97:626-30.